Blistering and flaking of amorphous alloys bombarded with He ions

HOU Ming-Dong, LIU Jie, ZHANG Qing-Xiang, LIU Gang

(*Institute of Modern Physics, the Chinese Academy of Sciences, Lanzhou 730000*)

Abstract The blistering and flaking behavior of many kinds of amorphous alloys under helium ion bombardment at room temperature was investigated. Helium ions with energies of 40 keV and 60 keV were implanted within the fluence range $(1.0\sim4.0)\times10^{18}$ ions/cm^2. The surface topography of samples after irradiation was observed by using a scanning electron microscope. The diameter of blister and the thickness of exfoliated blister lids were measured. The results showed that many kinds of surface topography characteristics appeared for different fluences, energies and amorphous alloys, such as flaking, blistering, exfoliation, blister rupture, second-generation blistering and porous structure. The dependence of surface damage modes and the critical fluence for the onset of blistering and flaking on the sort of materials and ion energy was discussed.

Keywords Blistering, Flaking, Exfoliation, Helium ion implantation, Amorphous alloy

CLC numbers O571.33, O756, TL62$^+$7

1 INTRODUCTION

The blistering and the exfoliation are serious surface erosion phenomena. They are regarded as main sources of the erosion of the first wall in a future fusion reactor. The erosion caused by the blistering and exfoliation is much larger than that due to the sputtering. The blister rupture can contaminate the plasma.

The blistering phenomenon would occur almost in various materials, including metal, alloy, semiconductor, ceramics and glass. The blistering phenomenon can be induced by the bombardment of not only inert gases, such as He, Ne, Ar, etc., but also active gases, such as H, D, etc. Therefore, investigation for the blistering phenomenon has important bearing on the fusion reactor technology and the related wide range of disciplines. The surface behavior of materials bombarded with high fluences of low energy ions has become a subject of particular interest[1]. A great number of investigations has been performed on blistering of crystalline metals and alloys by light ion bombardment. But the investigation on blistering of amorphous metals and alloys starts just lately. The blister and gas bubble formation in metallic glasses was first reported by Nandedkar and

Supported by the National Natural Science Foundation (19775058 and 10075064), Natural Science Foundation of Gansu Province (ZR96-025) and the Foundation of the Chinese Academy of Sciences (KJ952-S1-423)

Manuscript received date: 2000-03-27

Tyagi[2]. Up to now, the investigation of amorphous materials has not yet as perfect and systematic as that of crystalline materials in many respects.

Amorphous alloys, known as metallic glasses, exhibit improved mechanical and chemical properties[3,4] and are expected to have better radiation resistance. Before they were chosen as candidate material for application in fusion reactors, their blistering behavior must be understood. In the present work, the surface damage under helium ion bombardment for many kinds of amorphous alloys including binary, tribasic and polybasic alloy has been investigated. Amorphous alloys having different component and content are conducive to studying the dependence of surface topography on material properties. Particularly, many authors consider that metal-metal glasses may have better prospects for reactor applications because they generally have a relatively higher crystallization temperature and lower thermal neutron capture cross-section. The glasses of the Ni-Nb and Cu-Zr system studied in the present work are important in reactor technology.

2 EXPERIMENTAL

Metallic glasses, having the nominal compositions $Fe_{18.5}Ni_{55.5}B_{26}$, $Fe_{37.5}Ni_{37.5}B_{25}$, $Fe_{61.5}Ni_{20.5}B_{18}$, $Fe_{77}Ni_5B_{18}$, $Ni_{78}B_{14}Si_8$, $Fe_{77}B_{16}Si_5Cr_2$, $(Co_{94}Fe_4Cr_2)_{78}Si_8B_{14}$, $Ni_{60}Nb_{40}$, $Cu_{35}Zr_{65}$ and $Cu_{43}Ti_{57}$ were used in this study. The original metallic glasses were in the form of a ribbon of about $40\mu m$ thick. Samples of 2mm×2 mm size were cut from these ribbons. The samples were then polished using different grades of carborundum papers and finally with alumina paste. The samples were washed ultrasonically with acetone and then with distilled water. The samples were mounted on a water-cooled sample holder which was movable. During the irradiation the targets were kept at about 300 K.

The specimens were irradiated in high vacuum by helium ions with energies of 40 keV and 60 keV and to various fluences ranging from 1.0×10^{18} to 4.0×10^{18} ions/cm^2. The stability of helium ion energy was better than 0.1%. The ion beam created a circular spot of 3 mm in diameter and was sweeping so that the homogeneity was better than 95%. The average current densities for 40 keV and 60 keV were $4.2\mu A/cm^2$ and $3.2\,\mu A/cm^2$, respectively. After the irradiation, the samples were examined for surface topography by a JEM-1200EX type scanning electron microscope (SEM).

3 RESULTS AND DISCUSSIONS

SEM observation results for ten sorts of amorphous alloys studied in the work are listed in Table 1. Because determination of critical fluence for onset of blistering and flaking needs in-situ observation, the critical fluence given in Table 1 are only a range in which the critical fluence was situated. It can be seen from Table 1 that with the increase in fluence, various surface damage, such as flaking, blistering, exfoliation, blister rupture, second-generation blistering etc., appeared in succession under the irradiation of 40 keV and 60 keV for each amorphous alloy studied. But there was markedly difference in starting moment and development degree of every phenomenon for different materials.

Table 1 Surface damage mode of amorphous alloys irradiated with different fluences of He

Sample	Ion energy/keV	The critical fluence $/\times10^{18}$ions·cm^{-2}	Surface damage mode at different fluences/ $\times10^{18}$ions·cm^{-2}					
			1.0	1.5	2.0	2.5	3.0	4.0
$(Co_{94}Fe_4Cr_2)_{78}Si_8B_{14}$	60	0.5~1.0	B	B	F(B)	F(B)	F(B,E,F)	F[B,E(B),F(B)]
	40	0.5~1.0	F,B	F(B)	F(B,E)	F(B,E)	F[F(B),E(B)]	F[F(B),E(B)]
$Fe_{37.5}Ni_{37.5}B_{25}$	60	0.5~1.0	B	B	F	F(B,E)	F(B,E,F)	F[E(B),F(B)]
	40	0.5~1.0	B, F	F(B)	F(B,E)	F(B,E,F)	F[E(B),F(B)]	F[E(B),F(B)]
$Fe_{18.5}Ni_{55.5}B_{26}$	60			B	F		F(B,E,F)	F[E(B),F(B)]
	40			F(B)	F(B,E)		F(B,E,F)	F[E(B),F(B)]
$Fe_{77}Ni_5B_{18}$	60	0.5~1.0	B	F	F(B)	F(B,E)	F(B,E,F)	F[F(B),E(B)]
	40	0.5~1.0	F, B	F(B)	F(B,E)		F[F(B),E(B)]	F[F(B),E(B)]
$Fe_{61.5}Ni_{20.5}B_{18}$	60	0.5~1.0	B	B	F(B)	F(B,E)	F(F,B,E)	F[F(B),E(B)]
	40	0.5~1.0	F, B	F(B)	F(B,E)	F(B,F)	F[F(B),E(B)]	F[F(B),E(B)]
$Ni_{78}B_{14}Si_8$	60	0.5~1.0	B	B	F	F(B,E)	F(F,B)	F[F(B),E(B)]
	40	0.5~1.0	B, F	F(B)	F(B,E)	F(B,F)	F[F(B),E(B)]	F[F(B),E(B)]
$Fe_{77}B_{16}Si_5Cr_2$	60	0.5~1.0	B	B	F(B)	F(B,E)	F(B,E,F)	F[F(B),E(B)]
	40	0.5~1.0	B	F(B)	F(B,E)	F(B,E,F)	F[F(B),E(B)]	F[F(B),E(B)]
$Ni_{60}Nb_{40}$	60	1.0~1.5	×	F	F(B)	F(B,E)	F(F,B)	F[F(B),E(B)]
	40	1.0~1.5	×	F(B), B	F(B,E)	F(E,B)	F[E(B),F]	F[F(B),E(B)]
$Cu_{35}Zr_{65}$	60	1.0~1.5	×	F	F(B,E)	F(E,B)	F(E,F)	F[F(B),E(B)]
	40	1.0~1.5	×	F(B,E)	F(B,E)	F(B,E)	F(E,F)	F[F(B),E(B)]
$Cu_{43}Ti_{57}$	60				F(B,E)		F(B,E)	F(F E)
	40				F(B,E)		F[F,E(B)]	

B-blistering F-flaking, E-exfoliation, F(B)-blistering on the surface after flaking, E(B)-blistering on the surface after exfoliation, F(B,E,F)-blistering, exfoliation and the second flaking on the surface after flaking, F[F(B),E(B)]-the third generation blisters formed after exfoliation and/or the second flaking, ×-no significant surface damage, Blank-no sample

3.1 Blistering

As an example, the surface damage of amorphous alloy $Fe_{77}B_{16}Si_5Cr_2$ irradiated with 40 keV and 60 keV helium ions at room temperature is given as follows. As shown in Fig.1 (a) and (b), when the total fluence was 1.0×10^{18} ions/cm^2, the erosion mode on original surface was blistering for 40 keV and 60 keV bombardment. These were first-generation blisters, which were generally dome-shaped. The blister size was observed to increase with projectile energy for the same total fluence and flux. The average diameters were 0.74 mm for 40 keV irradiation and 1.03 mm for 60 keV irradiation, respectively. The corresponding blister densities were approximately 4.2×10^6 and 3.8×10^6 blisters/cm^2.

When *the total fluence was* 1.5×10^{18} *ions/cm*^{2}, *more dense* dome-shaped blisters were observed on the original surface for 60 keV irradiation. But for 40 keV irradiation, blisters on the second layer surface (flaked regions) were also observed. These second-generation blisters were generally not well dome-shaped. Typical surface for 40 keV and 60 keV irradiation to a total fluence 2.0×10^{18} ions/cm^2 is given in Fig.1(c) and 1(d). Blistering on the original and the second layer were seen together over the same sample for 60 keV irradiation. Exfoliation and blister rupture began to appear for 40 keV irradiation. When the total fluence was 2.5×10^{18} ions/cm^2, blister rupture and exfoliation were observed for 60 keV irradiation. Some third-generation blisters were formed on the third layer surface (regions left by exfoliation and ruptured blisters) for 40 keV irradiation.

As the total fluence increased to 3.0×10^{18} ions/cm^2, the third-generation blisters were generally seen throughout the third layer for 40 keV irradiation (Fig.1(e)). The third layer surface became larger without third-generation blisters on it for 60 keV irradiation (Fig.1(f)).

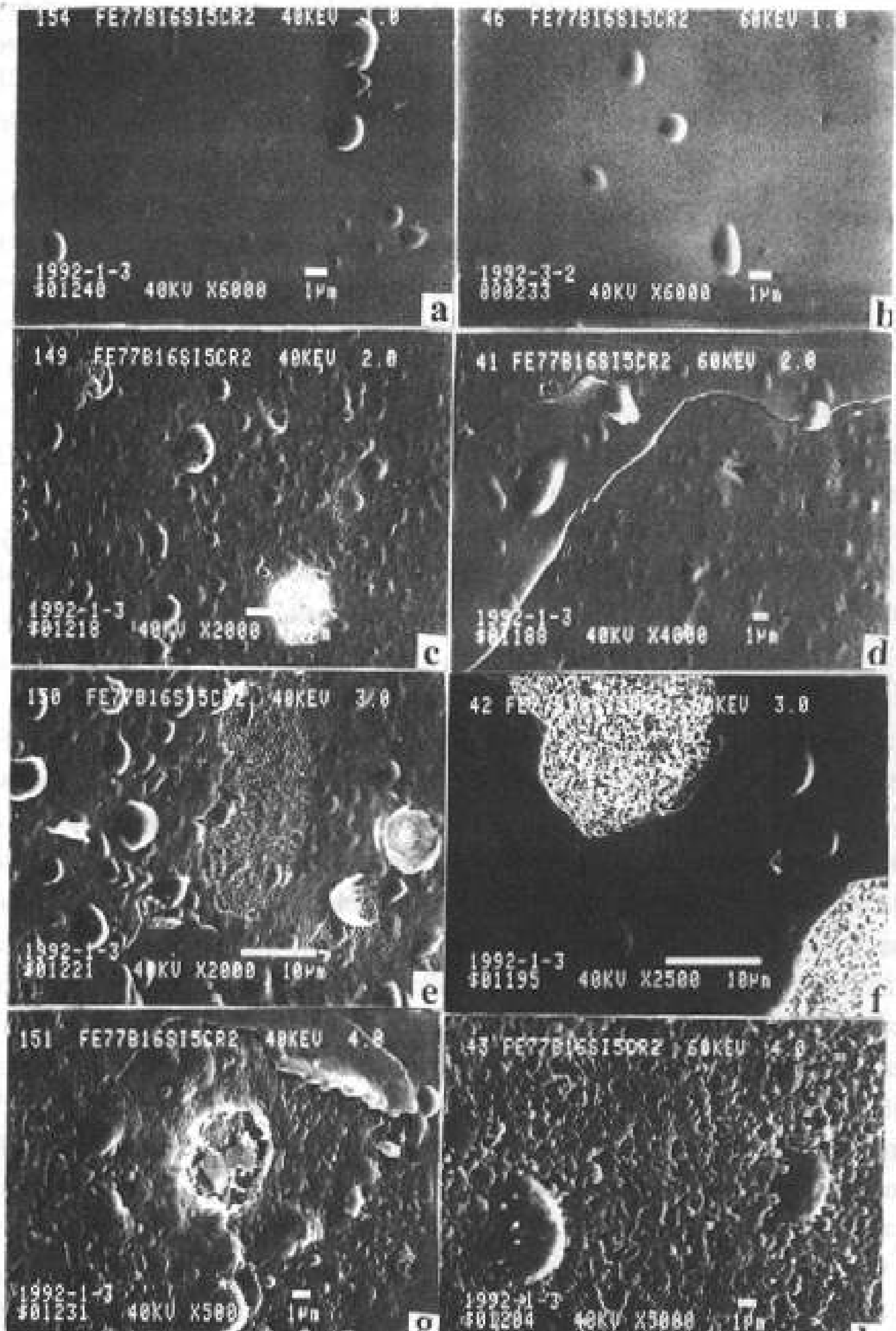

Fig.1 Typical SEM micrographs of amorphous alloy $Fe_{77}B_{16}Si_5Cr_2$ bombarded with helium ions:
(a) 40 keV, 1.0×10^{18} ions/cm^2, (b) 60 keV, 1.0×10^{18} ions/cm^2,
(c) 40 keV, 2.0×10^{18} ions/cm^2, (d) 60 keV, 2.0×10^{18} ions/cm^2,
(e) 40 keV, 3.0×10^{18} ions/cm^2, (f) 60 keV, 3.0×10^{18} ions/cm^2,
(g) 40 keV, 4.0×10^{18} ions/cm^2, (h) 60 keV, 4.0×10^{18} ions/cm^2

When the total fluence was 4.0×10^{18} ions/cm^2, nearly over the whole bombarded area the third-generation blisters were formed for 40 keV and 60 keV irradiation, but the blister density of the former was larger than that of the latter. The surface of these blisters were generally rougher and most of these blisters were not well dome-shaped (Fig.1(g) and 1(h)).

According to the above observations, it was seen the fact that the damage process under 40 keV ion irradiation was similar to that under 60 keV ion irradiation, but the evolution for 40 keV irradiation was more rapid than that for 60 keV irradiation.

3.2 Flaking and exfoliation

Fig.2 shows the typical surface topography of flaking for amorphous alloys $Fe_{61.5}Ni_{20.5}B_{18}$, $Fe_{37.5}Ni_{37.5}B_{25}$, $Ni_{78}B_{14}Si_8$ and $Ni_{60}Nb_{40}$ after 40 keV helium ion irradiation. There were flaked regions and unflaked regions on the same sample. The borders of flaked regions were irregular and not oriented. The flaked areas were large-scale. Compared with the original surface, the surface of the flaked region was rougher. In the flaked regions, there were pit-shaped and burst blisters, of which the density and size were similar to those of the blisters in unflaked regions. SEM observations showed that the critical fluence of flaking for amorphous $Ni_{60}Nb_{40}$ was the highest among those of the amorphous alloys used in this study.

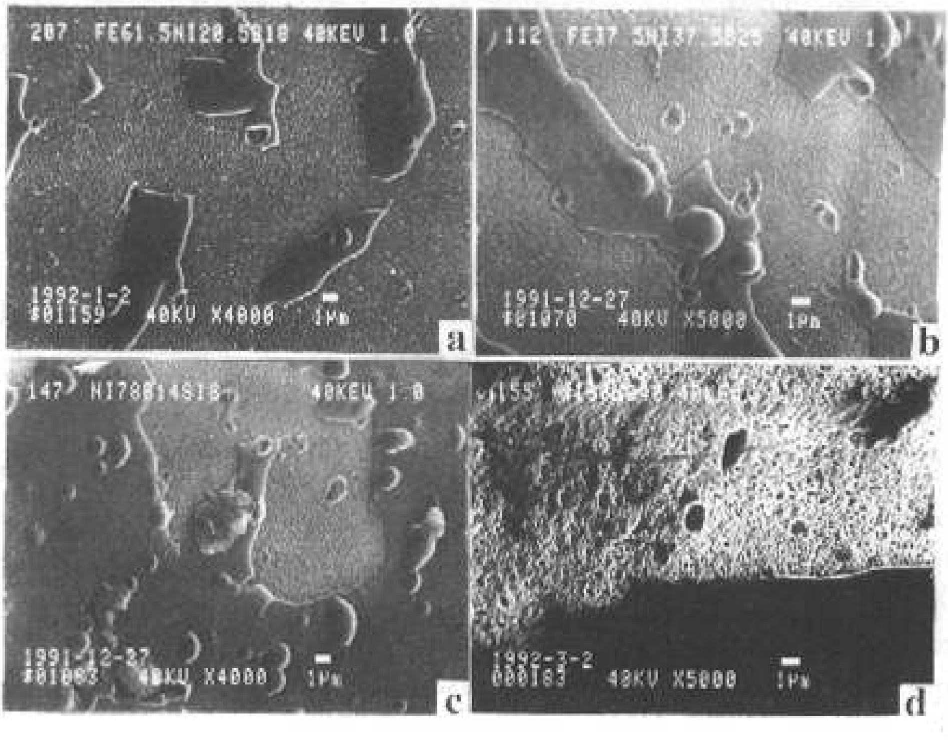

Fig.2 SEM micrographs of typical flaking topography for amorphous alloys irradiated with 40 keV helium ions:
(a) $Fe_{61.5}Ni_{20.5}B_{18}$, 1.0×10^{18} ions/cm^2, (b) $Fe_{37.5}Ni_{37.5}B_{25}$, 1.0×10^{18} ions/cm^2, (c) $Ni_{78}B_{14}Si_8$, 1.0×10^{18} ions/cm^2, (d) $Ni_{60}Nb_{40}$, 1.5×10^{18} ions/cm^2

With increase of the total fluence, a main mode of surface erosion was the exfoliation on the second layer surface. Fig.3 shows typical exfoliation behavior for four sorts of amorphous alloys at a fluence of 3×10^{18} ions/cm^2. The surface of exfoliated regions was even rougher than that of flaked regions. In the exfoliated regions, there were relatively flat areas, of which the shape, size and density were comparable to those of blisters in unexfoliated regions. The flat areas were the trace of the exfoliated blisters. Among these flat areas there were the very rough network regions. The borders of the exfoliated regions were irregular circles, and the area of the exfoliated regions was generally larger than that of a single blister.

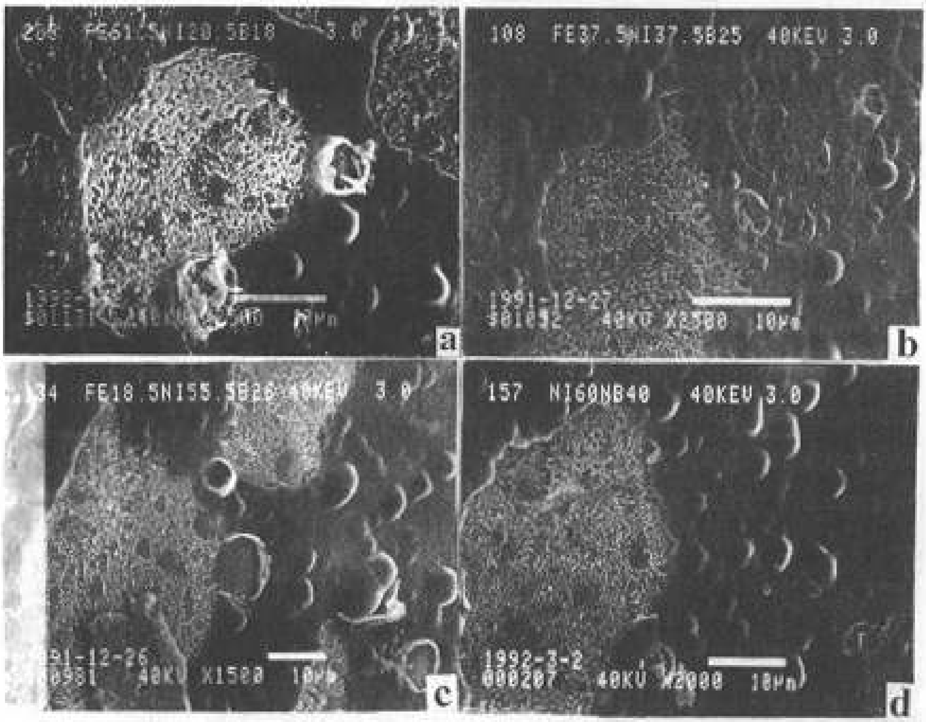

Fig.3 SEM micrographs of typical exfoliation topography for four sorts of amorphous alloys irradiated with 40 keV helium ions to 3.0×10^{18} ions/cm^2:
(a) $Fe_{61.5}Ni_{20.5}B_{18}$, (b) $Fe_{37.5}Ni_{37.5}B_{25}$, (c) $Fe_{18.5}Ni_{55.5}B_{26}$, (d) $Ni_{60}Nb_{40}$

From the above results we infer that under the present experimental conditions flaking is the main mode of surface erosion on the original surface. Flaking and blistering are two independent and competitive mechanisms. Flaking can occur not only in some regions with blisters, but also in some regions without blisters. On the second layer surface, a main mode of surface erosion is exfoliation, the mechanism of which is also different from that of flaking. The dense blisters at some regions are a prerequisite for exfoliation.

3.3 Blister rupture

Blister rupture can cause plasma contamination in future fusion reactor. As celestial body also would die, blister rupture is an inevitable end-result of evolution for every blister. SEM observation showed that blister rupture was one of the surface erosion modes on the second layer surface (flaked regions). The fluence for the onset of blister rupture was found to increase with the increase of ion energy. Among the amorphous alloys used in the present study, blister rupture erosion on $Cu_{35}Zr_{65}$ was most serious. For example, the ruptured blisters accounted for about (10~20)% of the total blisters on $Cu_{35}Zr_{65}$, only a few blisters ruptured on $Fe_{37.5}Ni_{37.5}B_{25}$ and $Ni_{78}B_{14}Si_8$, and the blister rupture was not observed on $Ni_{60}Nb_{40}$ and $Fe_{77}B_{16}Si_5Cr_2$ at the total fluence of 1.5×10^{18} ions/cm^2 for 40 keV irradiation.

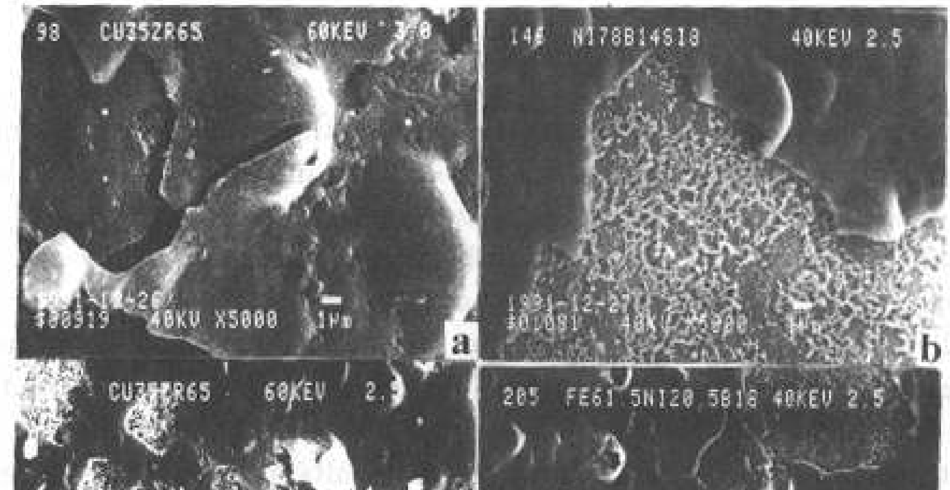

Fig.4 SEM micrographs of typical blister rupture for amorphous alloys irradiated with He: (a) $Cu_{35}Zr_{65}$, 60 keV, 3.0×10^{18} ions/cm^2, (b) $Ni_{78}B_{14}Si_8$, 40 keV, 2.5×10^{18} ions/cm^2, (c) $Cu_{35}Zr_{65}$, 60 keV, 2.5×10^{18} ions/cm^2, (d) $Fe_{61.5}Ni_{20.5}B_{18}$, 40 keV, 2.5×10^{18} ions/cm^2, (e) $Fe_{37.5}Ni_{37.5}B_{25}$, 40 keV, 3.0×10^{18} ions/cm^2, (f) $Fe_{37.5}Ni_{37.5}B_{25}$, 40 keV, 2.5×10^{18} ions/cm^2

Fig.4(a) and 4(b) show that an exfoliated region caused blisters on its border to rupture. But the most common mode was that blisters themselves often ruptured at the top rather than at the bottom. Fig.4(c) and 4(d) illustrates that the blister lid could be ruptured to form several irregular pieces, and cracks were observed on these pieces. Fig.4(e) is a typical SEM micrograph of a ruptured blister. The base of the ruptured blister was flat, but not smooth. On the base, particularly near the edge of the base, rough and cellular topography was clearly seen. Some pin-holes were also observed throughout the base. Fig.4(f) shows that the rough structure on the inner side of a blister lid was similar to that on the blister base. It is noted that ruptured blisters could be very large in size. For example, the largest diameter observed on $Cu_{35}Zr_{65}$ was about 20 μm at the total fluence of 2.5×10^{18}ions/cm^2 for 40 keV and 60 keV irradiation.

3.4 Blister mechanism

Helium, an inert gas, can be considered as essentially insoluble in all metals. The He ions impinging on the solid surface are slowed down in the material and then come to rest within the range distribution. The helium atoms are trapped in radiation-induced vacancies and precipitate into small gas bubbles with increasing fluence of irradiation. The presence of gas in bubbles and blisters has been confirmed by many experiments[5,6]. It is generally agreed in all models that blister formation is preceded by the nucleation of a microcrack near the implantation depth. Blistering is initially attributed to a sudden coalescence of bubbles. The matter of debate is, however, the mechanism for subsequent bulging of the overlaying implanted layer, which results in blistering. The gas-pressure model[7] holds that the gas pressure within the microcrack is responsible for the plastic deformation of the overlaying implanted layer. The thickness of the blister covers is approximately the same as the mean range of the implanted inert gas. The stress-model maintains[8,9], on the other hand, that the large compressive lateral stress induced in the implanted layer leads to elastic instability and buckling of the overlaying implanted layer. The major driving force for blister formation is stress release and not the gas pressure. Therefore, blister covers finally will break off at a depth where the stress has its maximum, but not the concentration of implanted ions. The thickness of the blister covers can be much larger than the calculated mean range of the implanted ions in amorphous materials. In the present work, the thickness of the blister covers has been measured by using a SEM for amorphous $Fe_{37.5}Ni_{37.5}B_{25}$, $Fe_{18.5}Ni_{55.5}B_{26}$, $Fe_{77}B_{16}Si_5Cr_2$, $Cu_{35}Zr_{65}$. The results show that the blister cover thickness after the correction for linear swelling is in agreement with the projected range of He ions within the experimental tolerance. It implies that the present result supports the gas-pressure model.

4 CONCLUSION

The surface erosion phenomena depend intensely on the parameters of not only projectile ion (sort, energy, fluence, flux), but also target material (composition, mechanical properties, surface roughness, temperature). From this work, following conclusions can be drawn.

(1) The critical fluence for metal-metal amorphous alloys $Ni_{60}Nb_{40}$ and $Cu_{35}Zr_{65}$ (about $(1.0\sim1.5)\times10^{18}$ ions/cm^2) is higher than that of metal-metalloid amorphous alloys studied in this work (about $(0.5\sim1.0)\times10^{18}$ ions/cm^2).

(2) With increase in the total fluence, the modes of surface damage as blistering, flaking, exfoliation are repeated and a trend of periodical surface erosion may exist. In this work, three generation blistering and two generation flaking have been observed for the fluence ranging from 1.0×10^{18} to 4.0×10^{18} ions/cm^2.

(3) With increase in the ion energy, the degree of the surface damage decreases. In a other words, the critical fluence increases with increase of the ion energy. Therefore, the surface damage for 40 keV always is more serious than that for 60 keV for the same fluence.

(4) The measured thickness of blister lid is in agreement with the projected range of helium ions within the experimental accuracy. This suggests a gas-pressure model for the blistering mechanism.

References

1 Roth J. In: Applications of Ion Beams to Materials, eds. Carter G, Colligon J S, Grant W A. London and Bristol: Institute of Physics, 1975, 280-292

2 Nandedkar R V, Tyagi A K. Rad Eff Letters, 1981, **58**:91-96

3 Cahn R W. Contemp Phys, 1980, **21**:43-75

4 Chen H S. Rep Prog Phys, 1980, **43**:353-432

5 Holt J B, Bauer W, Thomas G J. Radiat Effects, 1971, **7**:269-275

6 Daniels R D. J Appl Phys, 1971, **42**:417-419

7 Kaminsky M, Das S K. Radiat Effects, 1973, **18**:245-252

8 Behrisch R, Bøttiger J, Eckstein W *et al.* Appl Phys Lett, 1975, **27**:199-201

9 Roth J, Behrisch R, Scherzer B M U. J Nucl Mater, 1974, **53**:257-266